

01 Aug 2003

## FDTD Modeling of Isotropic Dispersive Magnetic Materials

Jing Wu

Marina Koledintseva

Missouri University of Science and Technology, [marinak@mst.edu](mailto:marinak@mst.edu)

James L. Drewniak

Missouri University of Science and Technology, [drewniak@mst.edu](mailto:drewniak@mst.edu)

David Pommerenke

Missouri University of Science and Technology, [davidjp@mst.edu](mailto:davidjp@mst.edu)

Follow this and additional works at: [https://scholarsmine.mst.edu/ele\\_comeng\\_facwork](https://scholarsmine.mst.edu/ele_comeng_facwork)



Part of the [Electrical and Computer Engineering Commons](#)

---

### Recommended Citation

J. Wu et al., "FDTD Modeling of Isotropic Dispersive Magnetic Materials," *Proceedings of the IEEE International Symposium on Electromagnetic Compatibility (2003, Boston, MA)*, vol. 2, pp. 904-909, Institute of Electrical and Electronics Engineers (IEEE), Aug 2003.

The definitive version is available at <https://doi.org/10.1109/ISEMC.2003.1236729>

This Article - Conference proceedings is brought to you for free and open access by Scholars' Mine. It has been accepted for inclusion in Electrical and Computer Engineering Faculty Research & Creative Works by an authorized administrator of Scholars' Mine. This work is protected by U. S. Copyright Law. Unauthorized use including reproduction for redistribution requires the permission of the copyright holder. For more information, please contact [scholarsmine@mst.edu](mailto:scholarsmine@mst.edu).

# FDTD modeling of isotropic dispersive magnetic materials

**Jing Wu**

ECE Dept. University of Missouri-Rolla, MO, USA  
jingwu@umr.edu

**Marina Y. Koledintseva**

ECE Dept. University of Missouri-Rolla, MO, USA  
marinak@ece.umr.edu

**James L. Drewniak**

ECE Dept. University of Missouri-Rolla, MO, USA  
drewniak@ece.umr.edu

**David J. Pommerenke**

ECE Dept. University of Missouri-Rolla, MO, USA  
davidjp@ece.umr.edu

## Abstract

*Numerical analysis using the finite-difference time-domain (FDTD) algorithm with a piecewise linear recursive convolution (PLRC) procedure for linear isotropic dispersive magnetic materials is presented. The frequency dependence of susceptibility used for this algorithm is represented in Debye, narrowband Lorentzian, and wideband Lorentzian forms, depending on the ratio of the resonance frequency and the resonance line width. Some numerical examples along with measurements are provided.*

## Keywords

FDTD modeling, piecewise linear recursive convolution, Lorentzian and Debye dispersion, magnetic materials, Ni-Zn ferrite, complex permeability, complex permittivity, small perturbation theory.

## INTRODUCTION

The finite difference time domain (FDTD) technique has been widely used to analyze electromagnetic phenomena. The FDTD method is based on the direct time integration of Maxwell's partial differential equations using the central finite difference method. The FDTD method is typically implemented with constant values of permittivity and conductivity. However, it does not allow accurate transient calculations to be made for materials with significant frequency dependence in their constitutive parameters. There are several approaches for incorporating dispersive media into the standard Yee FDTD algorithm. One approach uses recursive convolution (RC) of constitutive parameters and corresponding field components in the time domain [1,2]. Another approach is based on discretization of an auxiliary differential equation (ADE) [3]. In the approach proposed by Sullivan, the Z-transform is applied to Maxwell's equations to update field equations in the FDTD algorithm [4]. The piecewise linear recursive convolution (PLRC) method [5, 6] provides accuracy that rivals the ADE and Z-transform approaches, yet retains the speed, memory, and multiple advantages of the RC approach.

Herein, the PLRC method is used to incorporate dispersive magnetic media into FDTD. However, the frequency dependence of the permeability must be a "well-behaved" function having a causal inverse Fourier (or Laplace) transform, which contains a sum of complex exponentials

of time with constant coefficients. The simplest for linear isotropic magnetic material is a Debye model

$$\chi_{\mu}(jf) = \frac{A}{1 + j(f/f_{rel})}, \quad (1)$$

where  $A$  is a resonance amplitude parameter depending on the type of the magnetic material and proportional to its static magnetic susceptibility, and  $f_{rel} = \frac{1}{2\pi\tau_r}$  is the

relaxation frequency related to the Debye constant  $\tau_r$ . The dependency (1) is associated with domain walls movement in magnetic materials and describes a comparatively low-frequency (from RF to the lower part of microwave band) behavior of a dispersive medium [7,8]. At higher microwave frequencies resonance effects are associated with electron spin magnetic moment precession in ferro-, ferri-, and antiferromagnetic materials [7,8]. These resonance effects can be taken into account by a Lorentzian frequency dependence of the magnetic susceptibility,

$$\chi_{\mu}(jf) = \frac{A}{1 + j(f/f_{rel}) - (f/f_0)^2}, \quad (2)$$

where  $f_0$  is the resonance frequency,  $f_{rel} = f_0^2 / \Delta f$  is the relaxation frequency,  $\Delta f$  is the width of the Lorentzian resonance line at the -3 dB level, and  $A$  is a resonance amplitude parameter. The Debye and the Lorentzian models, both narrowband ( $2f_{rel}/f_0 < 1$ ) and wideband ( $2f_{rel}/f_0 > 1$ ), were introduced into the FDTD technique using the PLRC procedure [9].

## UPDATING EQUATIONS FOR FDTD MODELING OF MAGNETIC DISPERSIVE MEDIUM

The updating equation for the magnetic field in the linear isotropic magnetic dispersive medium is obtained in [9],

$$\vec{H}^{n+1} = \frac{1 - \xi^0}{1 + \chi^0 - \xi^0} \vec{H}^n - \frac{\Delta t}{\mu_0(1 + \chi^0 - \xi^0)} \nabla_d \times \vec{E}^{n+\frac{1}{2}} + \frac{1}{1 + \chi^0 - \xi^0} \Psi^n, \quad (3)$$

where the recursive convolution accumulator is

$$\Psi^n = (\Delta\chi^0 - \Delta\xi^0)\bar{H}^n + \Delta\xi^0\bar{H}^{n-1} + C_{rec}\Psi^{n-1}. \quad (4)$$

The constants  $\Delta\chi^0, \Delta\xi^0, C_{rec}$  have been derived in [9]. They are real-valued for the Debye media, and, in general, complex-valued for the Lorentzian media. If permittivity of the magnetic medium in the frequency range of interest is also frequency-dependent and follows the Debye or Lorentzian law, the electric field in the medium can be updated using the recursive convolution procedure, too, as in [10],

$$\begin{aligned} \bar{E}^{n+1} = & \frac{\epsilon_0\epsilon_\infty}{\epsilon_0(\epsilon_\infty + \chi_{e0}) + \sigma_e\Delta t} \cdot \bar{E}^n + \\ & + \frac{\epsilon_0}{\epsilon_0(\epsilon_\infty + \chi_{e0}) + \sigma_e\Delta t} \cdot \bar{\Phi}^n + \\ & + \frac{\epsilon_0\Delta t}{\epsilon_0(\epsilon_\infty + \chi_{e0}) + \sigma_e\Delta t} \cdot \nabla \times \bar{H}^{n+\frac{1}{2}}, \end{aligned} \quad (5)$$

where  $\epsilon_\infty$  is the optical region permittivity,  $\sigma_e$  is the d.c. conductivity of the dielectric,  $\chi_{e0}$  is static dielectric susceptibility depending on the dispersive law governing the susceptibility of the materials and found by integration

$$\chi_{e0} = \int_a^{\Delta t} \chi_e(\tau) d\tau. \quad (6)$$

Function  $\bar{\Phi}^n$  is a recursive convolution summation for the dielectric dispersion. It is real for the Debye and wideband Lorentzian cases, and complex for the narrowband Lorentzian case [11].

### COMPLEX PERMEABILITY MEASUREMENT

The FDTD modeling of the dispersive magnetic medium is tested herein with a specimen of a bulk Ni-Zn ferrite.

To model an electrodynamic structure containing this ferrite, the frequency dependencies of its constitutive parameters – permittivity and permeability – should be known. It is known, that the Debye or Lorentzian dispersive laws govern the frequency behavior of these parameters. The Debye or Lorentzian curves can be extracted from measurements using the methods discussed in papers [12,13].

Herein, the results of measuring the dispersive permeability of Ni-Zn ferrite are presented. A stripline resonator technique developed at NIST (USA) to measure the permeability of the specimen was applied [14].

The NIST stripline cavity is schematically shown in Figure 1. It consists of a centered conductor mounted equidistantly between two ground planes and terminated by two end plates. The end plates are permanently attached to the ground planes, thus the resonator is of fixed length and non-tunable.

The length of the resonator is 1 m, giving a fundamental resonance of approximately 150 MHz with harmonic resonances spaced at 150-MHz increments above the fundamental. The resonator upper frequency limit is defined by the frequency at which the first higher order TE<sub>10</sub> begins to propagate in the stripline cavity. For this cavity, the ground plane separation is 76.2 mm, giving a theoretical upper frequency limit of 1970 MHz. The *Q*-factor of the unloaded resonator has been several thousand after removing copper oxidation from its walls and applying silver paint to the joints to improve the conductivity of the structure.

A propagating TEM mode is excited within the stripline structure by the coupling loops mounted on one of the end plates. The first, or fundamental, resonance is achieved when the resonator length corresponds to a half-wavelength. There are higher-order resonances of the cavity at the harmonics of the fundamental frequency.

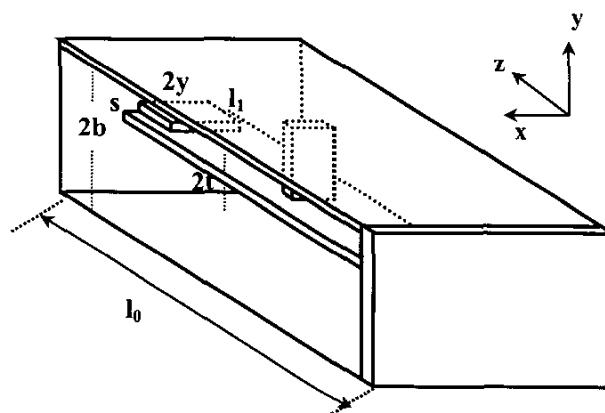
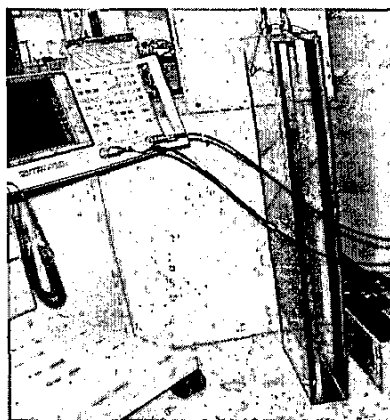


Figure 1. NIST stripline cavity for permittivity and permeability measurements.

Measurements of the complex magnetic permeability ( $\mu^* = \mu' - j\mu''$ ) are conducted by placing the specimen under test at an axial E-field node, located at the structure's end plates, where the electric field intensity is zero and does not influence on the measurement of permeability.

From Waldron's small perturbation theory [15], for a thin rectangular magnetic slab with  $2y$  in the x-direction,  $s$  in the y-direction, and  $l_1$  in the z-direction, the real and imaginary parts of permeability are found as

$$\mu'_r = 1 + \frac{\Delta f}{f_0} \frac{b(b-t)l_0}{Bysl_1} \quad (7)$$

$$\mu''_r = \left( \frac{1}{Q_L} - \frac{1}{Q_0} \right) \frac{b(b-t)l_0}{2Bysl_1}$$

In (7),  $2b$  is the distance between the cavity ground planes;  $t$  is the thickness of center conductor;  $l_0$  is the length of the resonator; and  $B$  is a geometry factor determined by the dimensions of the resonator [14,15]. The real and imaginary parts of permeability are measured by observing, respectively, the shift of the cavity resonance frequency  $\Delta f$  to the lower frequencies, and the decrease of the cavity  $Q$ -factor at the cavity loading with the sample under investigation.

Measured complex permeability data for the sample is shown in Figure 2. The results were checked to satisfy the causality principle, applying the Kramers-Kronig relations [16]. This means that the corresponding complex frequency characteristic of permeability is a rational function, and the time-domain susceptibility kernel, which is a pulse response of a medium, can be represented as a sum of complex exponential functions.

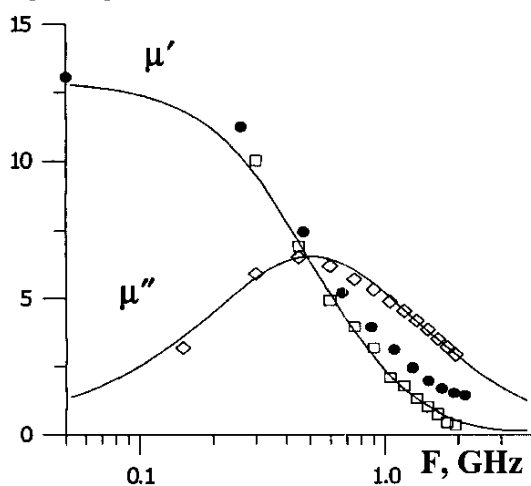


Figure 2. Real and imaginary parts of Ni-Zn ferrite permeability.

## COMPLEX PERMITTIVITY MEASUREMENT

Ni-Zn ferrite is a medium that has both dispersive permeability and permittivity in the frequency range of interest, up to 2 GHz. Hence, the FDTD modeling should include not only updating equations for magnetic field with recursive convolution term taking into account the dispersive law for magnetic susceptibility, but also for electric field taking into account the law for electric susceptibility.

The parameters of the dispersion law for the permittivity have been extracted from measurements. The real part of Ni-Zn ferrite permittivity was measured over the frequency range from 150 MHz to 2 GHz using the NIST's cavity method [14]. The rectangular specimen under test was placed in the region of maximum and uniaxial E-field, specifically, in the midpoint of the center strip, and with the smallest dimension oriented along the x-axis to minimize the E-field nonuniformity across the specimen. The H-field in the point where the ferrite specimen is placed is zero. Thus, the slab is located at the midpoint of the center strip in experiment. This measurement demonstrates that the permittivity of this sample can be approximated by the Debye dispersive curve. The imaginary part of the permittivity was reconstructed based on the Debye parameters extracted from the measurements of the real part of the permittivity.

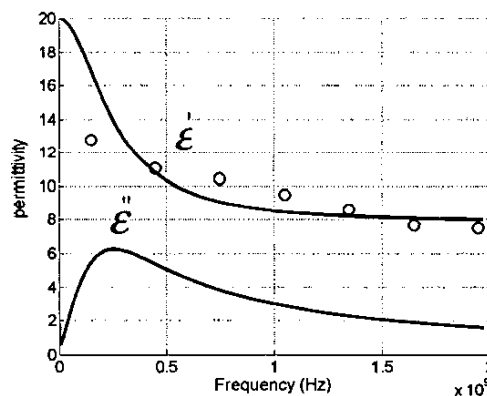


Figure 3. Real and imaginary parts of Ni-Zn ferrite permittivity.

## FDTD MODELING AND MEASUREMENTS OF A MICROSTRIP TEST FIXTURE WITH A NI-ZN FERRITE SUBSTRATE

The FDTD PLRC algorithm was applied to model a microstrip fixture comprised of two copper layers with an isotropic magnetic material spacer. The photograph of the fixture used in the experiments is shown in Figure 4.

The magnetic material is 31.4 mm long, 12.76mm wide and 3.24 mm thick. The upper copper tape is 6.32mm wide. Two MACOM SMA connectors are mounted on each end

of the microstrip line as test ports. The outer shields were soldered to the ground plane through two vertical copper-tape walls. The center conductor is soldered on microstrip line at each end. Four small corners were cut to prevent a short circuit of the microstrip line to the ground plane. Two port measurements were conducted using an HP 8753D network analyzer. The electrical lengths of the semi-rigid coaxial cables and SMA connectors were removed using the port extension feature of a full-path two-port calibration.

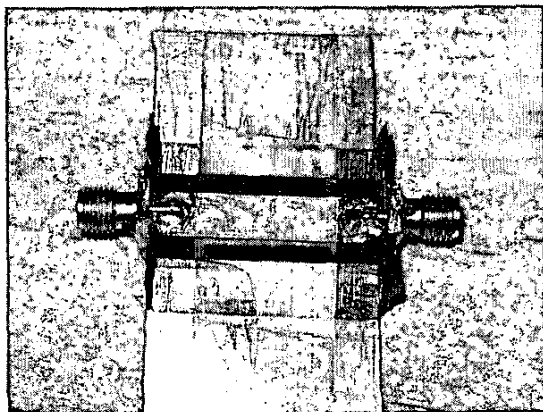


Figure 4. Microstrip fixture.

An orthographic view of the structure used in the FDTD modeling is shown in Figure 5. The basic computational domain in FDTD method consists of a rectangular mesh bounded by perfectly matched layers (PML) to simulate an infinite space. The computational domain was discretized by a uniform mesh of 0.316 mm × 0.324 mm × 0.316 mm along x, y, and z-axes, respectively, and the total number of cells was approximately 250,000. The strip and the ground plane were modeled as perfect electric conductors (PEC) 20 and 80 cells wide, respectively. The magnetic material layer between two adjacent planes was modeled with 10 cells thickness using PLRC algorithm. Two PEC plates were added vertically to model the copper tape at each side of the test fixture in experiment. A sinusoidal modulated Gaussian 50-Ohm voltage source was applied horizontally at Port 1 through a wire with 1 cell width, and Port 2 was terminated with a 50 Ohms load through a wire with 1 cell width. The wire structures were modeled using a thin wire algorithm.

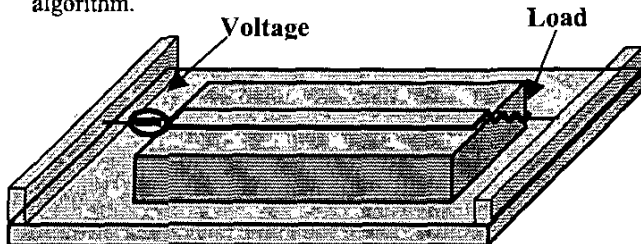


Figure 5. The configuration of the test fixture in FDTD modeling.

The standard Yee FDTD approach that incorporates the frequency-dependent loss of the media by a constant real value of effective conductivity and magnetic loss sigma in a number of individual frequency points was also used here. The effective conductivity  $\sigma_e^*$  and effective magnetic loss  $\sigma_m^*$  are introduced as

$$\begin{aligned} \nabla \times \vec{H} &= j\omega\epsilon_0\epsilon' \vec{E} + \sigma_e^* \vec{E}; \\ \sigma_e^* &= \omega\epsilon_0\epsilon'' + \sigma_e \end{aligned} \quad (8)$$

and

$$\begin{aligned} \nabla \times \vec{E} &= -(j\omega\mu_0\mu' \vec{H} + \sigma_m^* \vec{H}); \\ \sigma_m^* &= \omega\mu_0\mu'' \end{aligned} \quad (9)$$

As seen from (8) and (9), the effective conductivity and effective magnetic loss are frequency-dependent. By specifying a constant value of  $\sigma_e^*$ , the dielectric loss  $\epsilon''$  is included in the model using the normal Yee-algorithm updating equations. Similarly, by defining a constant value of magnetic loss  $\sigma_m^*$ , the imaginary part of permeability  $\mu''$  can be included in the model that uses the normal “non-dispersive” updating equations.

Ten uniformly distributed frequency “points” (actually, narrowband intervals with constant permeability and corresponding effective magnetic loss) were chosen within the frequency region from 100 MHz to 2GHz, as shown in Figures 6 and 7. The normal “non-dispersive” FDTD simulation was run independently 10 times for every chosen frequency “point”, and the corresponding S-parameters were obtained as a result of the simulations.

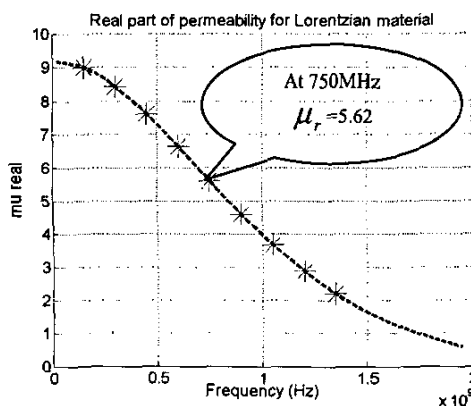


Figure 6. “Points” of  $\mu_r$  taken at the dispersive permeability curve for normal Yee’s algorithm.

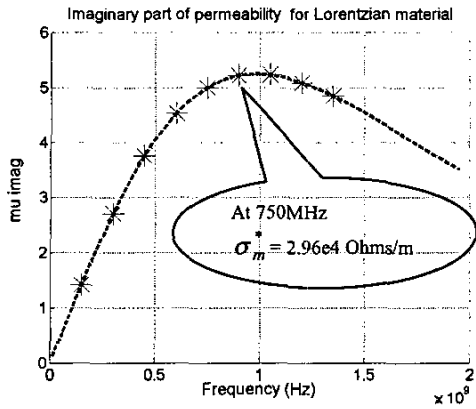
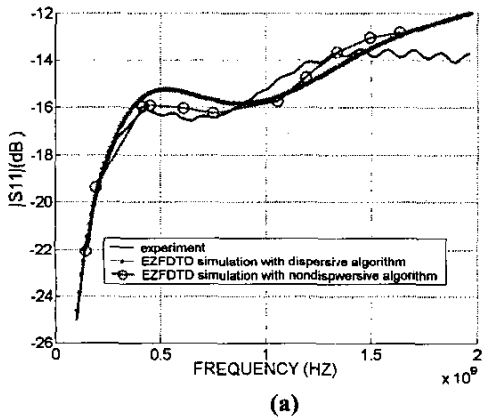
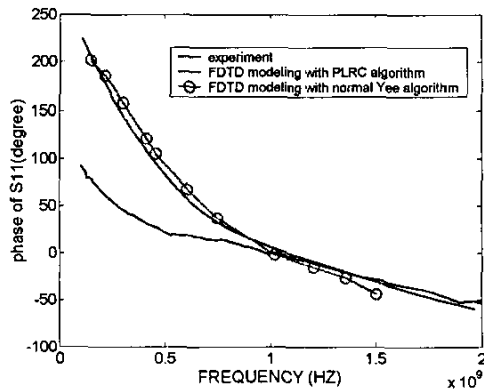


Figure 7. "Points" of  $\sigma_m^*$  taken at the dispersive permeability curve for normal Yee's algorithm.

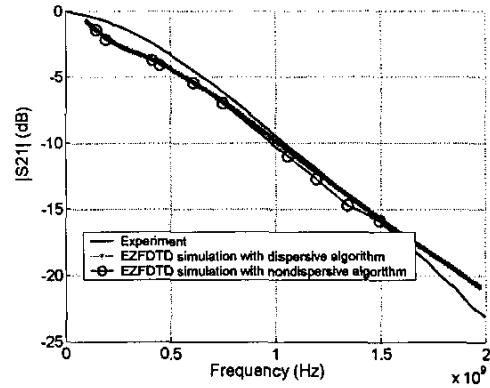
The modeled frequency dependencies for  $|S_{11}|$ ,  $|S_{21}|$ , and phases of  $S_{11}$  and  $S_{21}$  have been obtained using the PLRC algorithm, as well as the normal Yee-algorithm for the FDTD technique. The modeled and measured results are shown in Figure 8 (a-d).



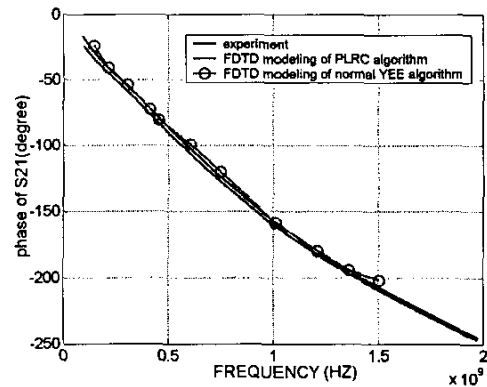
(a)



(b)



(c)



(d)

Figure 8. Measured and modeled S-parameters of the microstrip fixture with Ni-Zn substrate: (a) amplitude of  $S_{11}$ ; (b) phase of  $S_{11}$ ; (c) amplitude of  $S_{21}$ ; and (d) phase of  $S_{21}$ .

In general, there is a good agreement in the frequency range from 100 MHz to 2 GHz. The exception is discrepancy between the measured and modeled phase of  $S_{11}$  at lower frequencies. Probably, this is because the phase of  $S_{11}$  is more sensitive to the way the ports are modeled than the phase of  $S_{21}$ . As it was mentioned above, the geometry of the ports for modeling was simplified and reduced to 1-cell size.

### Summary and Conclusion

Numerical analysis using the finite-difference time-domain (FDTD) algorithm with a piecewise linear recursive convolution (PLRC) procedure for linear isotropic dispersive magnetic materials is presented. Good agreement was achieved between the modeled and measured results for a microstrip line structure with a magnetic dispersive material as a substrate. This demonstrates that the FDTD method incorporating the dispersive magnetic and dispersive dielectric medium is successful.

## ACKNOWLEDGMENTS

The authors of this paper thank Robert Johnk, Claude Weil, and Chriss Grosvenor for providing the NIST stripline cavity and magnetic material samples for experiments conducted at the UMR and for useful discussions. The authors would also like to thank Dr. Konstantin Rozanov (Russian Academy of Sciences) for valuable consultations.

## REFERENCES

- [1] K.S.Kunz and R.J.Luebbers, *The Finite Difference Time Domain Method for Electromagnetics*, Boca Raton, FL: CRC, 1993.
- [2] R.J.Luebbers, F.P.Hunsberger, K.S.Kunz, R.B.Standler, and M.Schneider, "A frequency-dependent finite-difference time-domain formulation for dispersive materials", *IEEE Trans. Electromagn. Compat.*, vol. 32, no. 3, pp. 222-227, Aug. 1990.
- [3] T.Kashiva and I.Fukai, "A treatment by the FDTD method of the dispersive characteristics associated with electronic polarization", *Microwave & Optical Technologies Letters*, v. 3, pp.203-205, June, 1990.
- [4] D.M.Sullivan, "Frequency-dependent FDTD methods using Z transforms", *IEEE Trans. Antennas Propagat.*, v. 40, pp.1223-1230, Oct.1992.
- [5] A.Taflove and S.Hagness, *Computational Electrodynamics: The Finite-Difference Time-Domain Method*. 2<sup>nd</sup> ed., Norwood, MA: Artech House, 2000.
- [6] D.V.Kelley and R.L.Luebbers, "Piecewise Linear Recursive Convolution for Dispersive Media Using FDTD", *IEEE Trans. Antennas Propagat.*, v. 44, no. 6, pp. 792-797, June 1996.
- [7] C.Kittel, *Introduction to Solid State Physics*, 2<sup>nd</sup> ed., Boca Raton, FL: CRC, 1993.
- [8] D.D.Pollock, *Physical Properties of Materials for Engineers*, 2<sup>nd</sup> ed., Boca Raton, FL: CRC, 1993.
- [9] J. Wu, M. Y. Koledintseva, and J. L. Drewniak, "FDTD Modeling of Structures Containing Dispersive Isotropic Magnetic Materials", in *Proc. XI Int. Conf. Spin-Electronics and Gyrovector Electrodynamics*, December 20-23, 2002, Firsanovka, Moscow Region, publ. UNC-1, Moscow Power Eng. Inst. (Techn. Univ.), pp. 536-546.
- [10] X.Ye, M.Y. Koledintseva, M. Li, and J.L.Drewniak, "DC power-bus design using FDTD modeling with dispersive media and surface mount technology components", *IEEE Trans. Electromagn. Compat.*, vol. 43, no. 64, pp. 579-587, Nov. 2001.
- [11] M. Y. Koledintseva, D.J.Pommerenke, J. L. Drewniak, "FDTD Analysis of Printed Circuit Boards Containing Wideband Lorentzian Dielectric Dispersive Media", in *Proc. IEEE Int. Symp. Electromagnetic Compatibility*, Minnesota, Aug. 2002, vol. 2, pp. 830-833.
- [12] M.Y.Koledintseva, K.N.Rozanov, J.L.Drewniak, and G.Di Fazio, "Restoration of the Lorentzian and Debye Curves of Dielectrics and Magnetics for FDTD Modeling", in *Proc. EMC EUROPE 5th Int. Symp. Electromagnetic Compatibility* September 9-13, 2002, Sorrento, Italy, no. PD27, pp. 687-692.
- [13] M.Y.Koledintseva and G.Di Fazio, "Extraction of the Lorentzian and Debye parameters from measurement data in a few frequency points", in *Proc. 10<sup>th</sup> Int. Conf. Spin Electronics*, Nov. 2001, Moscow Region, Firsanovka, publ. UNC-1, Moscow Power Eng. Inst. (Techn. Univ.), pp. 530-542.
- [14] C.M.Weil, C.A.Jones, Y.Kantor, and J.H.Grosvenor, "On RF Material Characterization in the Stripline Cavity", *IEEE Trans. Microwave Theory Tech.*, vol. 48, pp.226-274, Feb.2000.
- [15] R.A.Waldron, "Theory of strip-line cavity for measurement of dielectric constants and gyromagnetic-resonance line-widths", *IEEE Trans. Microwave Theory Tech.*, vol. 12, pp.123-131, Jan. 1964.
- [16] L.D.Landau, E.M.Lifshitz, and L.P.Pitaevskii, *Electrodynamics of Continuous Media*, 2<sup>nd</sup> ed., Oxford, NY: Pergamon Press, 1984.